

# Dynamic Response of Sizes of Humic Acid-Kaolin-PACl Aggregates

Rome-Ming Wu<sup>1\*</sup>, Kuo-Jen Li<sup>1</sup> and Shang-Suan Sung<sup>2</sup>

<sup>1</sup>Department of Chemical and Materials Engineering, Tamkang University,  
Tamsui, Taiwan 251, R.O.C.

<sup>2</sup>Chemical Engineering Department, National Taiwan University,  
Taipei, Taiwan 106, R.O.C.

## Abstract

The most commonly used experimental techniques to monitor the aggregation kinetics and to characterize structures of aggregates are scattering of light, X-rays and neutrons. We investigated in this study the coagulation dynamics for the humic acid-kaolin-polyaluminium chloride (PACl) aggregates using small-angle light scattering techniques. The mean aggregates sizes without addition of humic acids were only mildly affected by the kaolin concentration. With the addition of humic acids, the floc sizes are slightly reduced. At 600 rpm, the average aggregates size was larger with lower fractal dimension, i.e., the aggregates were large and loose; at 800 rpm, the average size was smaller with higher fractal dimension, i.e., under high shear rates, the aggregates were small and compact.

**Key Words:** Dynamics, Flocculation, Fractal Dimension, Small-Angle Light Scattering, Size

## 1. Introduction

In drinking water plants, coagulants, such as poly-aluminium chloride (PACl), are dosed in the raw water to bring small particles into settleable flocs. Organic substances commonly exist in the natural aquatic environment. Removal of organic substances like humics had attracted both research and practical interests. Gibbs [1] noted that the coagulation rate among small particles is decreased by the presence of natural organic substances.

The humic substances, through the better coagulation efficiency with PACl than mineral particles, were proposed to yield a loose and weak floc in the humic-mineral suspension [2,3]. Moreover, the refluxed sludge flocs could readily adsorb humics [4–6]. These results indicate the significant role of humics-particle-PACl aggregates on the coagulation processes.

Sludge flocs are highly porous fractal-like aggregates composed of many primary particles [7,8]. An important parameter that characterizes a fractal object is the fractal

dimension,  $D$  (–), which corresponds to the space-filling capacity of an object. The mass  $M$  of a fractal object with fractal dimension  $D$  can be considered to be proportional to its diameter  $d_f$ .

$$M \propto d_f^D \quad (1)$$

where  $1 \leq D \leq 3$ . The aggregates generated in water and wastewater treatment processes exhibit fractal dimensions ranging from 1.4 to 2.8 [7].

Light scattering experiments are an important tool for determining the fractal dimension of small aggregates. Bushell et al. [9], Kyriakidis et al. [10], Jung et al. [11], and Guan et al. [12] used small-angle light scattering to study the structure of flocs. The light scattering technique involves measurement of light intensity  $I$  as a function of the wave vector,  $Q$ . This vector is defined as the difference between the incident and scattered wave vectors of the radiation beam in the medium. The magnitude of the wave vector can be approximated as follows:

$$|Q| = Q = \frac{4\pi n \sin(\theta/2)}{\lambda} \quad (2)$$

\*Corresponding author. E-mail: romeman@mail.tku.edu.tw

where  $n$ ,  $\theta$ , and  $\lambda$  are the refractive index of the medium (–), the scattered angle (–), and the wavelength of radiation in vacuum (m), respectively. In scattering theory, the scattering intensity  $I(Q) \propto F(Q)S(Q)$ , where  $F(Q)$  and  $S(Q)$  are the form factor and the structure factor, respectively. The form factor is related to the shape of the particle while the structure factor accounts for the inter-particle correlations describing the spatial arrangement of the particles. In the regime  $QR_p \gg 1$ , where  $R_p$  is the primary particle size,

$$I(Q) \propto Q^{-4} \quad (3)$$

which is Porod's law [13]. In the regime  $QR \ll 1$  (Guinier regime), the form factor  $F(Q)$  is roughly constant. If the inequality,

$$1/R \ll Q \ll 1/R_p \quad (4)$$

holds, then one obtains

$$I(Q) \propto Q^{-D} \quad (5)$$

Restated, the log-log plot of  $I$  versus  $Q$  from data collected in scattering tests exhibits a linear character with a slope of  $-D$ .

The humic-mineral-PACl aggregates normally exhibit a poor settleability and high supernatant turbidity [14]. This negative impact was commonly attributable to the loose floc structure induced by the strong interaction between humics and the mineral particles.

## 2. Experimental

The particle size distribution of the kaolin slurry was determined using a Micromeritics 5100C Sedigraph and found to be a relatively monodispersed distribution with a mean diameter of approximately 2.3  $\mu\text{m}$ . The solid density was determined using a Micromeritics Accupyc 1330 pycnometer and found to be 2,730  $\text{kg/m}^3$ . The kaolin slurry was prepared by mixing 500 ppm kaolin powder and  $10^{-2}$  mol/L  $\text{NaClO}_4$  in distilled water.  $\text{NaClO}_4$  was added to provide a high enough ionic strength to prevent interference of other ions that might be released from the kaolin particle surfaces. The alkalinity was fixed at 100 mg/L. The pH was adjusted to 7 using  $\text{HClO}_4$  and  $\text{NaOH}$ .

Humic acid (N: 10%, P: 5%, K: 6%, humic acid:

79%) was purchased from Merck (Taiwan). The acid was first dissolved in a solution at pH 12, after filtering with the 0.45  $\mu\text{m}$  membrane, the pH of filtrate was adjusted back to 7 for use. A fixed amount of humic solution was vigorously agitated with the weighed kaolin suspension for 24 h to reach equilibrium. Afterwards, the humic-kaolin suspensions were placed into a stirred tank. In each tests 50 ppm of PAC was injected into the stirred tank at 600 rpm for 1080 s and subsequently 800 rpm for 180 s, then 600 rpm for 180 s and 800 rpm for another 180 s, and the 600–800 changed rotation speed pairs were repeated for 3 times. When the rotation speed was lower than 400 rpm, settling effect was noticeable. Whereas the rotation speed was higher than 1000 rpm, flocs were fragile. Hence the 600–800 rpm were the parameters in the experiment. Each measurement took 6 s. A total of 450 measurements were made for each coagulation test over 0–2700 s. In dynamics tests the PAC was injected with the water samples continuously withdrawn by the small angle laser light scattering sizer (Malvern Mastersizer 2000). This sizer consists of a 2 mW He-Ne laser ( $\lambda = 632.8$  nm) as the light source, and an optic lens and photo-sensitive detectors. The scattered light was collected at angles between  $0.01^\circ$  and  $32.1^\circ$ . The Malvern sizer was also used to measure the aggregate size between 0.02–2000  $\mu\text{m}$ .

## 3. Results and Discussion

### 3.1 Coagulation Kinetics

Weitz et al. [15] observed two regimes of aggregation, namely fast and slow aggregation with gold colloids. The rapid aggregation was found to produce aggregates with a fractal dimension of 1.75 and to reveal power-law kinetics in the form of  $d_f \sim t^{1/D}$ , where  $t$  is time. On the other hand, the slow aggregation was found to result in clusters with  $D = 2.05$  and exhibit exponential kinetics with  $d_f \sim \exp(bt)$ , where  $b$  is a constant dependent on the experimental conditions.

Figure 1 depicts the coagulation kinetics in this study. The size growth function for all samples exhibit an exponential form, i.e., the slow aggregation and reaction limited control of aggregation (RLCA)[9,11,12,16]. (For simplicity, there were shown only three samples.)

### 3.2 Coagulation Dynamics

As previously described, dynamic coagulation tests were conducted by a mixer with different rotation speeds.

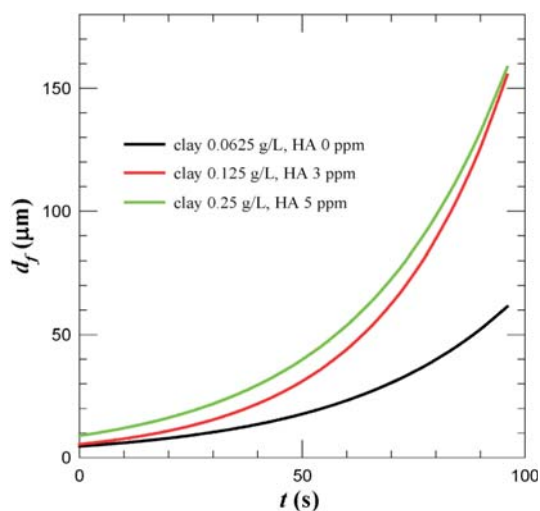


**Figure 1.** Size growth exponential function.

The steps were 600 rpm (0–1080 s), 800 rpm (1080–1260 s), 600 rpm (1260–1440 s), 800 rpm (1440–1620 s), 600 rpm (1620–1800 s), 800 rpm (1800–1980 s), 600 rpm (1980–2160 s), 800 rpm (2160–2340 s), 600 rpm (2340–2520 s), and 800 rpm (2520–2700 s). Figures 2 and 3 are the time evolution of aggregates sizes with coagulant PACl 50 and 200 ppm, respectively. The mean aggregates sizes without addition of humic acids were only mildly affected by the kaolin concentration. For example, the largest growth size for 0.0625 g/L, 0.125 g/L, and 0.25 g/L kaolin dosed with 50 and 200 ppm PACl were about 150  $\mu\text{m}$  (Figure 2a–2c) and 220  $\mu\text{m}$  (Figure 3a–3c), respectively.

With the addition of humic acids, the floc sizes are slightly reduced. For example, the mean sizes of 0.125 g/L kaolin added with 0, 3, 5, and 7 ppm humic acids and dosed with 50 ppm PACl (Figure 2b) at 500 s were 124, 105, 95, and 72  $\mu\text{m}$ , respectively. At high PACl dose, the size reduction effect was less obviously (162, 164, 162, and 149  $\mu\text{m}$ , Figure 3b). The reason is that the large amount of added coagulant (200 ppm) could compensate for the consumption with humic acids [14].

Owing to the effects of hydrodynamic shear the aggregates start to break up after the largest growth sizes. At 1080 s (800 rpm), the aggregates broke more seriously, at 1260 s (600 rpm), the aggregates restructured. The mean sizes of the “breakage-restruction” were shown in Figure 4. As the two dash lines illustrated in Figure 4a, it seems that there are two monotonously decreased curves, one for 600 rpm, the other for 800 rpm. It is reasonable to assume that under different hydrodynamic shear, the structure of the aggregates may be different. The fol-

lowing paragraph will demonstrate this viewpoint.

### 3.3 Floc Structure

Figures 5 and 6 summarize the time evolution of mean fractal dimension of the aggregates.

The value of fractal dimension vibrated up and down for each curve. In other words, each plot shown in Figures 5 and 6 could be viewed as two monotonously de-

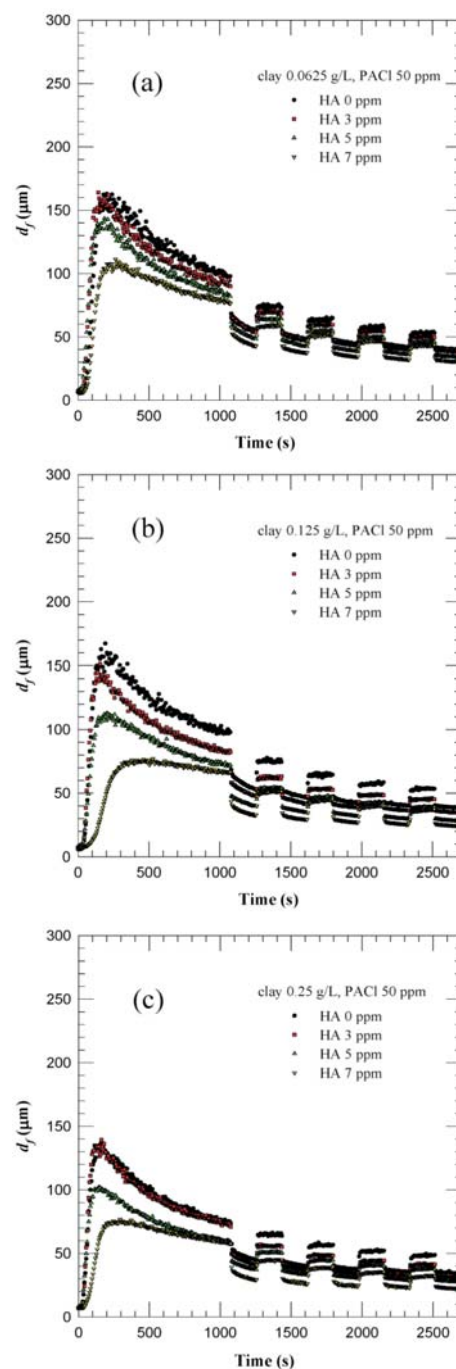


**Figure 2.** Time evolution of aggregate size (PACl 50 ppm).

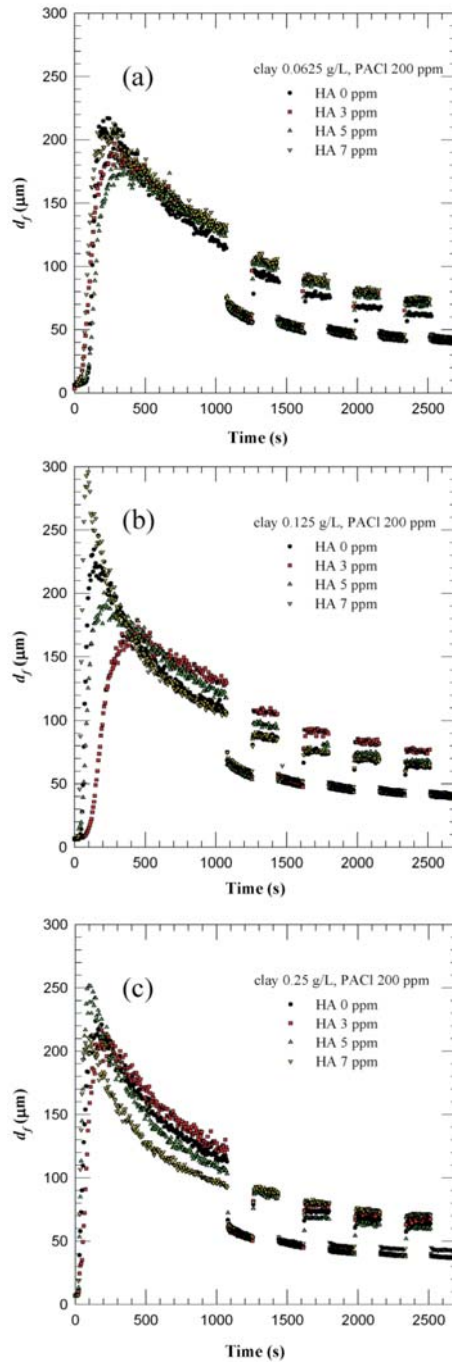


**Figure 3.** Time evolution of aggregate size (PACI 200 ppm).

creased curves, one for 600 rpm, and the other for 800 rpm. For example, the average fractal dimensions for 0.0625 g/L kaolin, 5 ppm humic acid, dosed with 50 ppm PAC (Figure 5a) were 2.14 and 1.85 at 800 and 600 rpm, respectively. The corresponding average sizes were 59 and 42 μm. Hence the above mentioned aggregates had two-level structures as Wu et al. reported [17]. The aggregates may have a small and compact core, surrounded

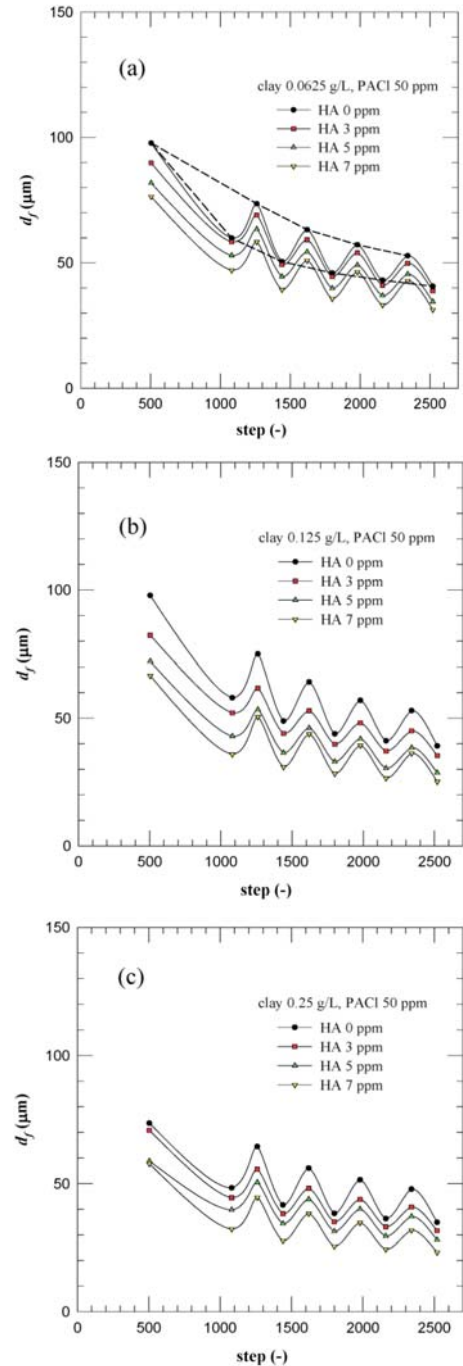


**Figure 4.** Time evolution of mean aggregate size (PACI 50 ppm).

by a large and loose macrofloc, making them a two-level structure. At 600 rpm, the average aggregate size was the larger 59 μm with lower fractal dimension 1.85, i.e., the aggregates were large and loose; at 800 rpm, the average size was the smaller 42 μm with higher fractal dimension 2.14, i.e., under high shear rates, the aggregates were small and compact. Jorand et al. [18] also proposed



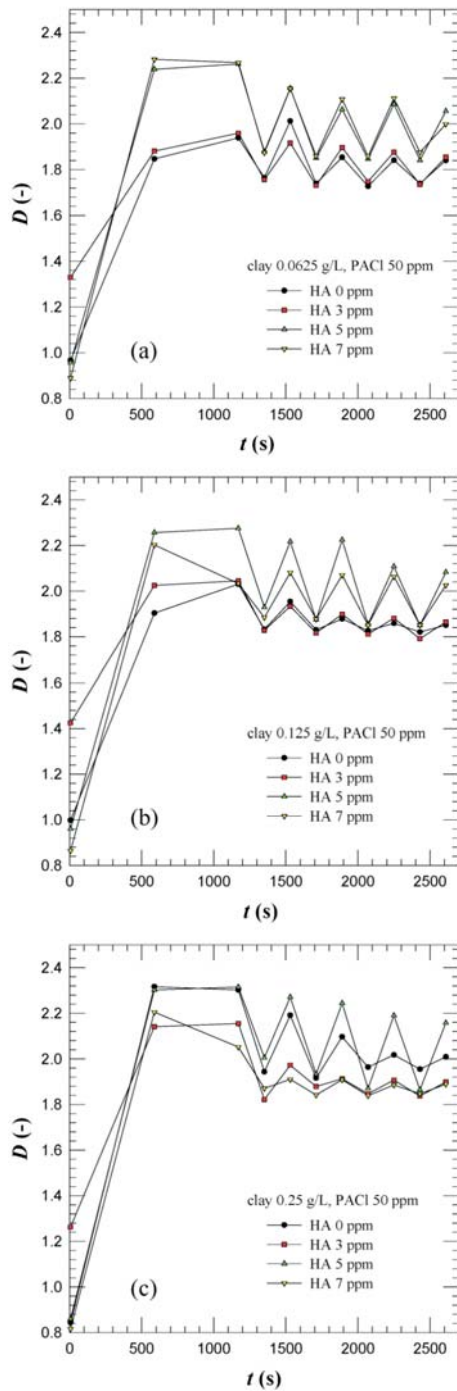


**Figure 5.** Time evolution of fractal dimension (PACl 50 ppm).

that macroflocs of size 125  $\mu\text{m}$  were made from 13  $\mu\text{m}$  microflocs and 2.5  $\mu\text{m}$  primary particles.

#### 4. Conclusion

With the assistance of the small-angle light scattering

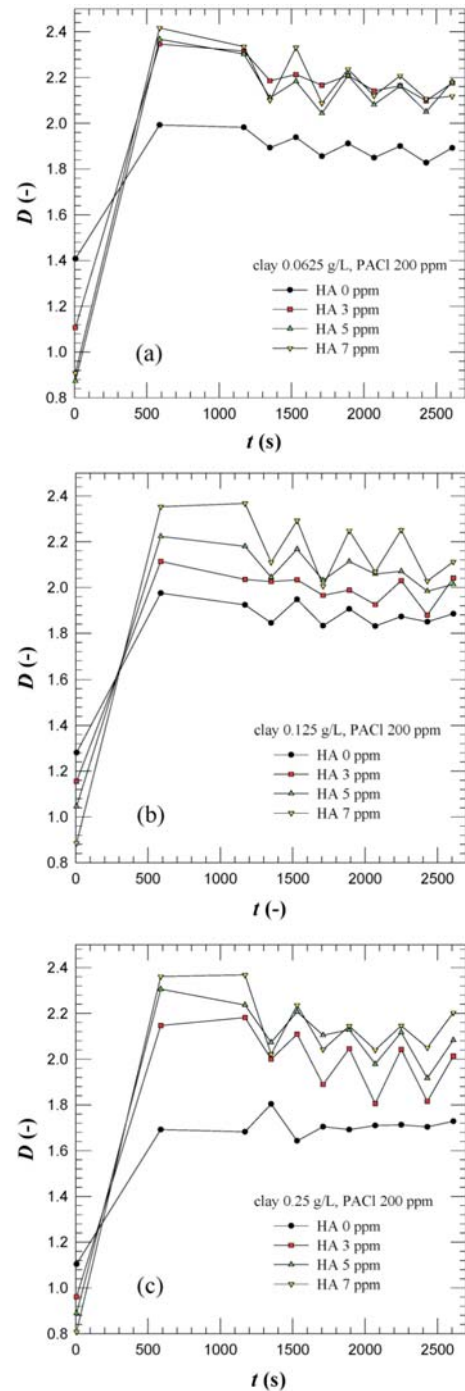


**Figure 6.** Time evolution of fractal dimension (PACl 200 ppm).

test, we investigated the coagulation dynamics of humic acid-kaolin-polyaluminium chloride (PACl) aggregates under defined hydrodynamic environment. Aggregates sizes evolution and the fractal dimension data were recorded. Growth of the aggregates making them had a small and compact core. The core or microfloc was then aggregated

by other particles making a large and loose macrofloc. Hence under high shear, the peripheral particles flaked off easily, leading to small and compact microfloc and turbid supernatant with high level of organic matter.

### Acknowledgement

National Science Council (NSC), ROC financially supported this work.

### Nomenclature

- $\lambda$  wavelength of radiation in vacuum, (nm)
- $\theta$  scattered angle, (rad)
- $b$  constant, (-)
- $d_f$  diameter of aggregate, ( $\mu\text{m}$ )
- $D$  fractal dimension, (-)
- $F(Q)$  form factor, (-)
- $I$  incident light intensity, ( $\text{m}^2$ )
- $M$  mass of aggregates, (kg)
- $n$  refractive index, (-)
- $Q$  wave vector, (-)
- $R$  size of aggregates, ()
- $R_p$  size of primary particles
- $S(Q)$  structure factor, (-)
- $t$  time, (s)

### References

- [1] Gibbs, R. J., "Effect of Natural Organic Coatings on the Coagulation of Particles," *Envir. Sci. Technol.*, Vol. 4, pp. 237–240 (1983).
- [2] Tambo, N. and Watanabe, Y., "Physical Characteristics of Floccs – I. The Floc Density Function and Aluminum Floc," *Wat. Res.*, Vol. 13, pp. 409–419 (1979).
- [3] Rebhun, M., "Floc Formation and Breakup in Continuous Flora Flocculation and in Contact Filtration," *Chemical Water and Wastewater Treatment*, Hahn, H.H. and Klute, R. (Ed.) Springer-Verlag, Berlin, pp. 117–126 (1990).
- [4] Mazet, M. and Angbo, L., "Adsorption of Humic Acids onto Performed Aluminum Hydroxide Floccs," *Wat. Res.*, Vol. 24, pp. 1509–1518 (1990).
- [5] Cathalifaund, G., Wais-Mossa, M. T. and Mazet, M., "Performed Ferric Hydroxide Floccs as Adsorbents of Humic Substances," *Wat. Res.*, Vol. 27, pp. 55–60 (1993).
- [6] Julien, F., Guerous, B. and Mazet, M., "Comparison of Organic Compounds Removal by Coagulation-Flocculation and by Adsorption onto Performed Hydroxide Floccs," *Wat. Res.*, Vol. 28, pp. 2567–2574 (1994).
- [7] Li, D. H. and Ganczarczyk, J., "Fractal Geometry of Particle Aggregates Generated in Water and Wastewater Treatment Process," *Envir. Sci. Tech.*, Vol. 23, pp. 1385–1389 (1989).
- [8] Jiang, Q. and Logan, B. E., "Fractal Dimensions of Aggregates Determined from Steady-State Size Distributions," *Environ. Sci. Technol.*, Vol. 25, pp. 2031–2038 (1991).
- [9] Bushell, G. C., Yan, Y. D., Woodfield, D., Raper, J. and Amal, R., "On Techniques for the Measurement of the Mass Fractal Dimension of Aggregates," *Adv. in Colloid Interface Sci.*, Vol. 95, pp. 1–50 (2002).
- [10] Kyriakidis, A. S., Yiantsios, S. G. and Karabelas, A. J., "A Study of Colloidal Particle Brownian Aggregation by Light Scattering Techniques," *J. Colloid Interface Sci.*, Vol. 195, pp. 299–306 (1997).
- [11] Jung, S. J., Amal, R. and Rpper, J. A., "The Use of Small Angle Light Scattering to Study Structure of Floccs," *Part. Part. Syst. Character.*, Vol. 12, pp. 274–278 (1995).
- [12] Guan, J., Waite, T. D. and Amal, R., "Rapid Structure Characterization of Bacterial Aggregates," *Environ. Sci. Tech.*, Vol. 32, pp. 3735–3742 (1998).
- [13] Mandelbrot, B. B., *The Fractal Geometry of Nature*. N.Y., U.S.A. (1983).
- [14] Lin, W. W., Sung, S. S., Lee, D. J., Chen, Y. P., Chen, D. S. and Lee, S. F., "Coagulation of Humic-Kaolin-PACl Aggregates," *Wat. Sci. Tech.*, Vol. 47, pp. 145–152 (2002).
- [15] Weitz, D. A., Huang, J. S., Lin, M. Y. and Sung, J., "Limits of the Fractal Dimension for Irreversible Kinetic Aggregation of Gold Colloids," *Physical Review Letters*, Vol. 54, pp. 1416–1419 (1985).
- [16] Kyriakidis, A. S., Yiantsios, S. G. and Karabelas, A. J., "A Study of Colloidal Particle Brownian Aggregation by Light Scattering Techniques," *J. Colloid Interface Sci.*, Vol. 195, pp. 299–306 (1997).
- [17] Wu, R. M., Lee, D. J., Waite, T. D. and Guan, J., "Multilevel Structure of Sludge Floccs," *J. Colloid Interf. Sci.*, Vol. 252, pp. 383–392 (2002).
- [18] Jorand, F., Zartarian, F., Thomas, F., Block, J. C., Bottero, J. Y., Villemin, G., Urbain, V. and Manem, J., "Chemical and Structural (2D) Linkage between Bacteria within Activated Sludge Floccs," *Wat. Res.*, Vol. 29, pp. 1639–1647 (1995).

**Manuscript Received: Sep. 29, 2006**

**Accepted: Nov. 6, 2006**